

Implementation of Improved Realtime Offline Image Filtering Method by Autocorrelation Function

M.A.Gopisaran,
 Government College of Engineering,
 Tirunelveli, TamilNadu, India.

S.S. Sreeja Mole
 Government College of Engineering,
 Tirunelveli, Tamil Nadu, India.

ABSTRACT

A novel scheme for anisotropic diffusion driven by the image autocorrelation function is implemented. The diffusion tensor field is estimate by autocorrelation and computation from a scalar product of diffusion tensor and the image Hessian functions obtains an evolution equation. For a minimized spatial support for a hessian a set of filters are proposed. The filtering method performs favorable in many cases in particularly at low noise levels. A real time performance is easily achieved in a GPU implementation.

Keywords

Adaptive filtering, diffusion filtering, image enhancement, steerable filters, structure tensor

1. INTRODUCTION

The efficient structure-preserving image denoising and enhancement is a relevant problem in many applications. The anisotropic extension of nonlinear diffusion using the structure tensor often leads to accuracy and particular close to lines and edges. Auto-correlation driven diffusion a novel variant of tensor-driven diffusion filtering proposes that 1) the system only requires a scalar product of diffusion tensor and Hessian in the evolution equation. 2) An equivalent to a particular instance of adaptive filtering and it is easy to implement in a fast numerical scheme.

Structure-preserving, denoising and enhancement are practical problems to be solved in many applications, e.g., image and video coding, digital cameras, and medical imaging. Most of these applications require a real-time approach, which limits the range of available methods. The numerical implementation of anisotropic diffusion is less trivial. Peak signal to noise ratios is check the accuracy of the filtering values.

Optimal results usually require estimates of image priors and have been analyzed and compared with the another filtering ratio values. Visual information fidelity(VIF) and structural similarity index(SSIM) used for the experimental evaluation methods. Further the tensor calculus, tensor representations, anisotropic extensions and iterated adaptive filtering method are valuate for calculate tensor field and auto-correlation function of time discrete function and stability of functions are going to implement.

2. NOVEL VARIANT OF TENSOR-DRIVEN DIFFUSION FILTERING

2.1 Tensor Calculus

The tensors are coordinate-system independent algebraic entities. The vector and the scalar products are denoted to represents the values.

The scalar product between two column vectors and is usually denoted by the matrix product of the transpose \mathbf{a} and \mathbf{b}

$$\langle \mathbf{A} | \mathbf{B} \rangle = \text{trace}(\mathbf{A}\mathbf{B}^T) = \sum_i \sum_j \mathbf{a}_{ij}\mathbf{b}_{ij}$$

Tensors will be often built by outer products of vectors .Since second-order tensors form a vector space, a scalar product (Frobenius product) is defined, which reads for two tensors. In most cases, we will consider symmetric tensors as the spectral theorem and allows a decomposition into real eigen values of the given values, where is an orthogonal matrix formed by the eigenvectors and the diagonal matrix containing the corresponding eigen values.

$$\mathbf{A} = \mathbf{O} \mathbf{\Lambda} \mathbf{O}^T = \mathbf{O} \text{diag}(\lambda_i) \mathbf{O}^T$$

$$\mathbf{A}^n = (\mathbf{O} \mathbf{\Lambda} \mathbf{O}^T)^n = \mathbf{O} \mathbf{\Lambda}^n \mathbf{O}^T = \mathbf{O} \text{diag}(\lambda_i^n) \mathbf{O}^T$$

\mathbf{O} is an orthogonal matrix formed by the eigenvectors of \mathbf{A} and $\mathbf{\Lambda}$ is the diagonal matrix containing the corresponding (real) eigenvalues

2.2 Tensor Representation

Tensor representations occur frequently and mostly for representing local orientation and the deviation from a simple signal model. The gradient-based structure tensor can be derived as the solution of a least-squares approach to fitting a simple signal model. Another alternative is to consider the structure tensor as an estimate of the Hessian of the autocorrelation function of the signal.

$$\Delta^T \mathbf{A} = \text{div}(\mathbf{A}) = \left(\sum_i \frac{\partial a_i}{\partial x_j} \right)_j$$

A symmetric function that might expand it as where denotes the Hessian operator with the

Introduction

Cooperative communication is one of the fastest growing areas of research, and it is likely to be a key enabling technology for efficient spectrum use in future. The key idea in cooperation is that of resource-sharing among multiple nodes in a network. The reason behind the exploration of user-cooperation is that willingness to share power and computation with neighboring nodes can lead to savings of overall network resources. Mesh networks provide an enormous application space for user-cooperation strategies to be implemented. In 3G wireless transmission the quality of multimedia signal suffers severe degradations due to effects like signal fading caused by multipath propagation. To reduce such effects, diversity is proposed that can be used to transfer the different samples of the same signal over essentially independent channels.

power theorem the values are obtain by the expectation value. This expectation value is usually estimated by locally weighted averaging the outer product of the image gradient and that the gradient operators in are normally regularized by some low-pass filter, that is using Gaussian derivatives. The local weight function is also mostly chosen as a Gaussian function for the structure tensor functions.

$$J(\mathbf{x}) = \int \omega(\mathbf{y}) \nabla \mathbf{b}(\mathbf{x} - \mathbf{y}) \nabla^T \mathbf{b}(\mathbf{x} - \mathbf{y}) d\mathbf{y}.$$

2.3. Anisotropic Extensions:

The diffusion scheme is defined as an evolution equation of an image over time as where is the diffusion tensor, which is computed by modifying the eigen values of the structure tensor . Applying the product rule and the divergence term is split into two parts of the diffusion functions.

If the structure tensor is computed by spatial averaging, the divergence of the diffusion tensor is nonzero in general and needs to be estimated. If the tensor is computed by averaging over the different dimensions of a vector-valued image and no spatial averaging is applied, the divergence term can be converted into a trace-based term. By modifying the evolution equation can be expressed by a single trace-based term and the divergence of the diffusion tensor is eliminated.

$$\frac{\partial \mathbf{b}}{\partial t} = \text{div}(D(J)\nabla \mathbf{b})$$

This elimination is impossible if the structure tensor is computed by spatial averaging. When implementing anisotropic diffusion, an iterative algorithm that updates the input image successively has to be implemented. In each time-step, the diffusion tensor and the image gradient have to be estimated. If the evolution is divergence-based, another numerical approximation of a derivative operator is required, which is applied to the product of diffusion tensor and gradient.

$$\text{div}(D(J)\nabla \mathbf{b}) = \text{div}(D(J)\nabla \mathbf{b}) + \text{trace}(D(J)H\mathbf{b})$$

Five sequential operations are required for the Diffusion tensors are :- Image gradients, point-wise products, local averaging, point-wise product, and gradient.

By the trace-based approach only four sequential operations are required for the final gradient and it is replaced with a second image derivative which can be computed in parallel to the diffusion tensor.

2.4. Iterated Adaptive Filtering

Adaptive filtering is main idea is to compose a spatially variant filter kernel by linear combinations of shift-invariant kernels. The linear coefficients are locally estimated by an orientation-dependent scheme. A comprehensible formulation of the method can be found in Adopting the notation, the filter is composed as where is an orientation-selective high-pass filter with orientation is the dual tensor for the orientation tensor . The high-pass filter with orientation is defined in the Fourier domain by a polar separable filter with radial component and an angular component. The dual tensors can be computed via the isometric vector representation and proportional to the negative Hessian, since The tensor-controlled adaptive filter scheme is often applied in an iterated way to achieve good denoising results and with a very small constant multiplier and selecting the low-pass filter appropriately as then it is possible to show that the iterated adaptive filtering implements a numerical scheme for autocorrelation-driven anisotropic diffusion.

$$\sum_k \tilde{N}_k \mathbf{H}_k \mathbf{p}_{ik} = \mathbf{u} \mathbf{u}^T$$

$$\mathbf{H}_{LP} = \mathbf{1} - \gamma \rho(|U|) = \mathbf{1} - \gamma |U|^2$$

3. AUTO-CORRELATION FUNCTION

The autocorrelation-driven anisotropic diffusion is defined by the evolution where is the diffusion tensor determined by the autocorrelation function at the current spatial position and functions starts with defining autocorrelation-driven diffusion filtering in the continuous domain, where the autocorrelation function estimate is inserted after computing the divergence and resulting in a purely trace-based formulation. This continuous equation is then discretized in the temporal

domain and the equivalence to iterated adaptive filtering is found. This Filtering is fully discretized, its stability is analyzed, and practical aspects are verified with the appropriate values

$$\frac{\partial \mathbf{b}}{\partial t} = \text{div}(\mathbf{B}(\mathbf{R})\nabla \mathbf{b})$$

3.1 Auto-Correlation Filtering:

Tensor-driven anisotropic diffusion use the structure tensor for controlling the diffusion process. Interpreting the structure tensor as an estimate of the autocorrelation function, one can go one step back and reformulate anisotropic diffusion with a diffusion tensor that depends on the autocorrelation function instead.

Definition 1: The autocorrelation-driven anisotropic diffusion is defined by the evolution where is the diffusion tensor determined by the auto-correlation function at the current spatial position. This definition is particularly sensible from a statistical point of view and consider to

ergodicity assumption which is essential for denoising by weighted spatial averaging. If the image signal is ergodic in a strict sense, all statistical moments are stationary and thus the autocorrelation is constant, resulting in unweighted averaging. If the image signal is structured, its statistical moments are not stationary. The autocorrelation function becomes highly peaked in all directions in this case. Averaging should only be performed orthogonal to the structure. The autocorrelation function is peaked along the structured direction and flat orthogonal to it.

$$\text{div}(\mathbf{B}(\mathbf{R})\nabla \mathbf{b}) = \langle \mathbf{B}(\mathbf{R}) | H \mathbf{b} \rangle$$

3.2 Time-Discrete Scheme For Autocorrelation-Driven Anisotropic Diffusion:

In filtering method, the continuous differential equation needs to be discretized in the spatial and temporal domain and its start with discretizing the temporal domain, Using a standard explicit scheme for time discretization and the upper limit for depends on the spatial discretization. The Hessian can be written in terms of a set of dual tensors and corresponding filters and plugging this into yields where we replaced . Sorting terms gives which is equivalent to an adaptive filtering according to with constant multiplier and the low-pass filter . This low-pass filter is the inverse Fourier transform.

$$\text{div}(D(J)) \neq 0.$$

3.3 Fully Discrete Scheme For Autocorrelation-Driven Anisotropic Diffusion:

Three filter sets have to be designed for the full discrete in the spatial system. They are Hessian, derivatives , and the averaging kernel has chosen to be a Gaussian function. The exact value for the variance is not crucial, as the experimental results do not differ for small variations. The derivatives used in the structure tensor and the second derivatives used to compute the Hessian are computed with filter masks of minimum size. This is motivated by an observation made in Reducing linear regularization that is using smaller filter masks, for the benefit of increased regularization of the structure tensor improves the overall result. In order to obtain small filter masks with good isotropy for that to apply a similar optimization strategy but with a different objective function. The optimal filter set in terms of and is obtained by minimizing the weighted angular error between two normalized tensors in the Fourier domain where is the 2-D frequency, are the Fourier transforms. The weighting function is determined by the weight in and the statistics of natural

images .It will minimize the resulting parameters and are given in good approximation in Sobel filter.

$$b_{t+1} = b_t + \gamma (Id - C(J)) | - \sum_k \tilde{N}_k h P_i k b t)$$

3.4 Stability Of The Discrete Scheme

The fully discrete scheme is rewritten in the form and the function is tested for six criteria and continuity in its argument, symmetry, unit row sums, nonnegative off-diagonals, irreducibility, and positive diagonal. Then derive a parametrized effective convolution kernel, which can then be converted into the corresponding matrix operator. Then need to specify the diffusivity function and it is known from the literature that the diffusivity determines the relation between nonlinear diffusion and robust estimation. The width of the influence function in robust estimation Is more important than the exact shape.

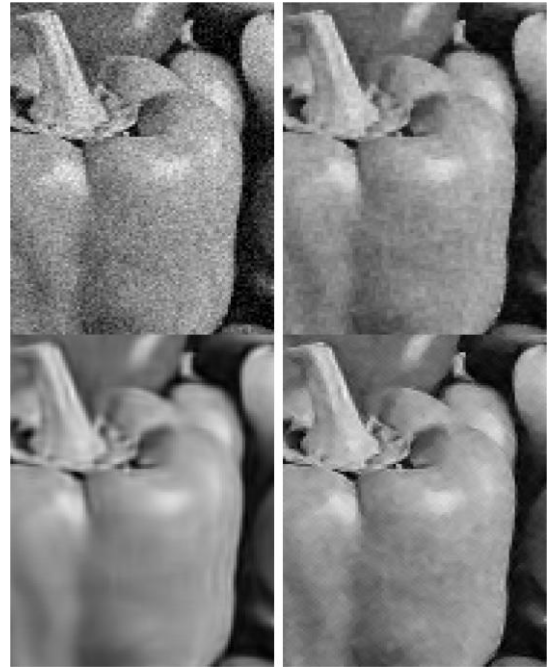
Let denote the eigenvalues of and the angle of the Eigenvector corresponding to discrete scheme . and the Positive diagonal entries are Obtained .If the off-diagonals are not nonnegative and notice to the upper left element in equals . Even though the nonnegativity is violated, This does not imply instability of the discrete scheme.we can compute the -intervals where the coefficients in become negative and these intervals are such that the angular distance to the gradient orientation is maximized, and it have a maximum level of integration in these sectors and due to the vanishing sums property, the resulting effective operator is nonnegative. For instance, if we integrate along the columns and obtain the weighted 1-D Laplacian operator .

3.5 Practical Details

The experienced as the most critical parameter of the algorithm in order to obtain comparative results is the width of the diffusivity function . Too large values of lead to blurred results that is structure is considered as noise, and too small values lead to noisy results, since noise is considered as structure.

The parameter that gives the statistically best discrimination of structure and noise can be derived from a null-hypothesis test and the resulting choice for is where is the estimated noise variance according to the method described in with a minor modification.

The parameter of anisotropic diffusion is the stopping time and implement to the iterations are stopped as soon as the image update is below a certain threshold. The threshold for the stopping criterion is empirically set to by looking at curves of maximum PSNR in logarithmic scale. However, this is only partly satisfying as the rate of change might depend on the image structure and not on the difference to a noise-free instance of the image.



the

Fig. 1. The pepper image points the filtering residue of the noise levels and the detecting edge level is maximized.

3.6 Quality Of Measures

The image been tested with PSNR,SSIM,VIF values and table be calculated. The graphical representations of the given plotted values shows the performance of the proposed system.



Fig 1 Test image of Lena from the Database it shows the PSNR, VIF, SIM results for the autocorrelation method . The values are to be iterated

PSNR SCORES:

Table 1 shows that Numerical Results of PSNR scores for the iterated σ values .

σ	Iteration 1	Iteration 2	Iteration 3	Iteration 4	Iteration 5	Iteration 6	Iteration 7	Iteration 8	Iteration 9	Iteration 10
1	47.7842	42.0257	37.5155	33.2045	32.0496	30.7879	29.7974	26.2692	22.9069	20.2905
2	47.7704	42.0015	37.8385	32.8609	31.3235	30.1625	29.2555	25.5357	22.4419	20.4588
5	47.7770	42.0231	37.5063	33.4843	31.2988	29.8639	29.2257	25.5118	23.1873	20.6576
10	47.7786	42.9360	37.0078	32.8758	31.3311	30.4002	29.4509	25.6978	22.6603	20.4609
15	47.7814	42.9386	37.7027	34.3516	31.8524	30.6126	30.0628	25.8919	23.0600	20.4830
20	47.7817	42.0157	37.7111	34.0058	31.8653	30.1807	29.4795	25.8962	22.6868	20.4827
25	47.7808	42.0179	36.9957	32.8568	30.8568	29.8667	30.1312	25.7074	22.8595	20.6663
50	47.7830	42.9324	36.9943	32.8481	32.2299	30.9410	30.1504	25.7035	23.0275	20.6651
75	47.7919	42.5523	37.9643	34.5049	31.6217	30.6341	29.8225	25.8924	22.6925	20.5146
100	48.1698	43.1747	37.9450	33.2052	31.3210	30.1574	29.2502	26.0483	22.7063	20.5193

VIF SCORES:

Table 5.2 shows that Numerical Results of VIF scores for the iterated σ values .

σ	Iteration 1	Iteration 2	Iteration 3	Iteration 4	Iteration 5	Iteration 6	Iteration 7	Iteration 8	Iteration 9	Iteration 10
1	1.0003	1.0006	0.9926	0.9854	0.9613	0.9382	0.9152	0.7425	0.6563	0.5644
2	1.0000	1.0002	0.9890	0.9850	0.9667	0.9452	0.9230	0.7717	0.6648	0.5534
5	0.9998	0.9997	0.9905	0.9793	0.9643	0.9464	0.9201	0.7665	0.6325	0.5409
10	1.0000	0.9981	0.9929	0.9836	0.9649	0.9363	0.9164	0.7611	0.6543	0.5507
15	1.0002	0.9987	0.9907	0.9749	0.6925	0.9397	0.9043	0.7664	0.6564	0.5676
20	1.0000	0.9999	0.9899	0.9766	0.9600	0.9438	0.9169	0.7524	0.6502	0.5429
25	1.0000	1.0000	0.9931	0.9840	0.9688	0.9482	0.8959	0.7604	0.6454	0.5421
50	1.0000	0.9982	0.9930	0.9838	0.9539	0.9289	0.8957	0.7569	0.6361	0.5390
75	1.0003	0.9997	0.9889	0.9733	0.9663	0.9410	0.9142	0.7619	0.6623	0.5587
100	0.9991	0.9973	0.9875	0.9821	0.9655	0.9438	0.9214	0.7444	0.6494	0.5443

SSIM SCORES:

Table 5.3 shows that Numerical Results of SIM scores for the iterated σ values.

σ	Iteration 1	Iteration 2	Iteration 3	Iteration 4	Iteration 5	Iteration 6	Iteration 7	Iteration 8	Iteration 9	Iteration 10
1	0.9983	0.9935	0.9792	0.9395	0.9128	0.8787	0.8459	0.6914	0.5313	0.4159
2	0.9983	0.9935	0.9806	0.9357	0.90003	0.8641	0.8300	0.6590	0.5168	0.4274
5	0.9983	0.9936	0.9795	0.9434	0.9013	0.8591	0.8308	0.6569	0.5460	0.4360
10	0.9983	0.9945	0.9770	0.9357	0.9001	0.8692	0.8352	0.6645	0.5224	0.4235
15	0.9982	0.9944	0.9798	0.9511	0.9083	0.8733	0.8533	0.6715	0.5394	0.4253
20	0.9983	0.9983	0.9799	0.9475	0.9087	0.8635	0.8350	0.6722	0.5234	0.4250
25	0.9983	0.9935	0.9771	0.9361	0.8953	0.8583	0.8580	0.6660	0.5322	0.4333
50	0.9982	0.9945	0.9769	0.9354	0.9152	0.8815	0.8564	0.6632	0.5375	0.4309
75	0.9983	0.9941	0.9813	0.9536	0.9056	0.8752	0.8469	0.6742	0.5256	0.4283
100	0.9984	0.9948	0.9813	0.9401	0.9012	0.8652	0.8312	0.6813	0.5251	0.4274

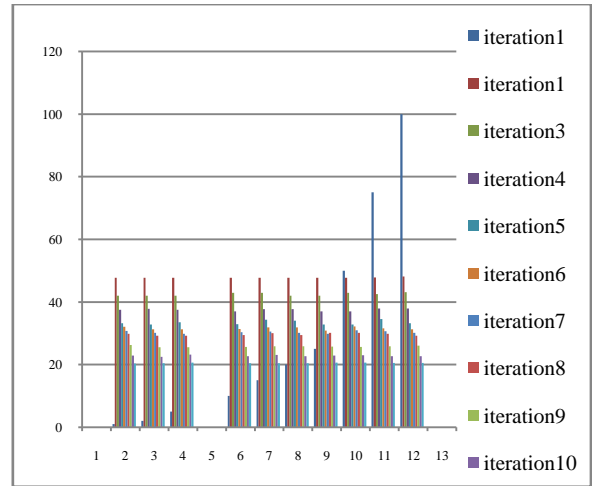


Fig 2 Shows PSNR values of the test image and iterations of the σ values.

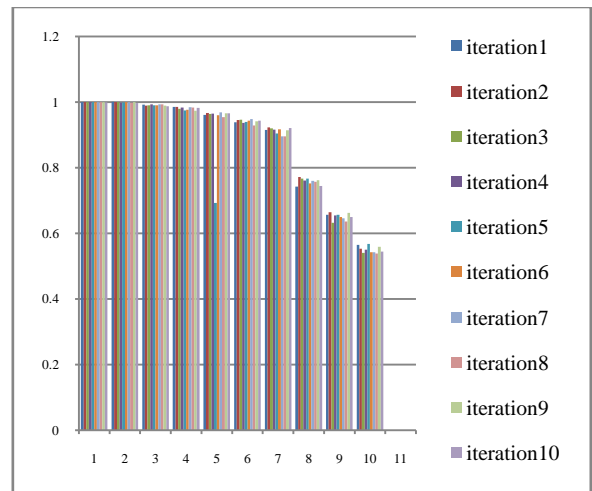


Fig 3 Shows VIF values of the test image and iterations of the σ values.

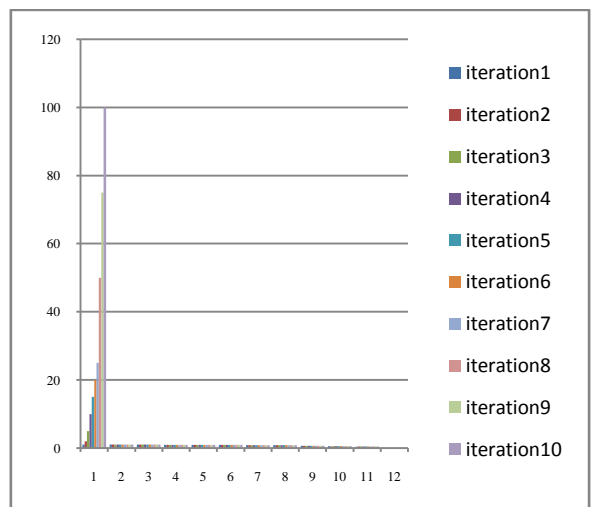


Fig 4 Shows SSIM values of the test image and iterations of the σ values.

The graphical representations of the PSNR, VIF, SSIM values plotted and the noise level ratios of the each iterated values are differed in the shown figures. The noise level reduced by the sequence iterated σ values and values been increased.

The low noise levels for the finger prints and edge detection be highly performed by the driven diffusion functions. The proposed method works better than the fields of expert except for the three highest noise levels, the house image, and the medium to high level noise in the pepper image.

4. CONCLUSION

The autocorrelation is to define tensor-driven diffusion based on the autocorrelation function. This scheme is equivalent to a special case of adaptive filtering. Then an optimized filter setup for the computation and compare the method with GSM, BM3D, and EEDF using three quality measures, PSNR, VIF, and SSIM. The result of the comparison is ambivalent in the way that the ranking of methods depends on the choice of the quality measure, the noise level, and the kind of image. GSM and BM3D for low-noise cases and images with many line structures. Compared with EEDF, the autocorrelation driven filtering is clearly superior, except for the VIF scores. Graphically of the diffusion results contain fewer artifacts than the GSM results. This scheme is easy to implement and fast to execute. So that our autocorrelation driven diffusion filtering is a good choice in many practical denoising tasks.

5. FUTURE WORKS

The auto-correlation functions are implement for real time frames of video system. The frames are extracted from motion pictures and the iterated filtering functions applied to detect the noise levels and edge detection can be performed.

6. REFERENCES

- [1] C. Tomasi and R. Manduchi, "Bilateral filtering for gray and color images," in *Proc. 6th ICCV*, 1998, pp. 836–846.
- [2] Y. Cheng, "Mean shift, mode seeking, and clustering," *IEEE Trans. Pattern Analysis and Machine Intell.*, vol. 17, no. 8, pp. 790–799, Aug. 1995.
- [3] D. Comaniciu and P. Meer, "Mean shift: A robust approach toward feature space analysis," *IEEE Trans. Pattern Anal. Mach. Intell.*, vol. 24, no. 5, pp. 603–619, Apr. 2002.
- [4] M. Felsberg and G. Granlund, "Anisotropic channel filtering," in *Proc. 13th Scand. Conf. Image Anal.*, 2003, pp. 755–762, ser. LNCS 2749.
- [5] J. Portilla, V. Strela, J. Wainwright, and E. P. Simoncelli, "Image denoising using scale mixtures of Gaussians in the wavelet domain," *IEEE Trans. Image Process.*, vol. 12, no. 11, pp. 1338–1351, Nov. 2003.
- [6] M. Elad and M. Aharon, "Image denoising via sparse and redundant representations over learned dictionaries," *IEEE Trans. Image Process.*, vol. 15, no. 12, pp. 3736–3745, Nov. 2006.
- [7] R. A. Carmona and S. Zhong, "Adaptive smoothing respecting feature directions," *IEEE Trans. Image Process.*, vol. 7, no. 3, pp. 353–358, Mar. 1998.
- [8] M. Felsberg, "On the relation between anisotropic diffusion and iterated adaptive filtering," in *Proc. DAGMSymp. Mustererkennung*, 2008, vol. 5096, pp. 436–445.
- [9] J. Bigün and G. H. Granlund, "Optimal orientation detection of linear symmetry," in *Proc. IEEE 1st Int. Conf. Comput. Vis.*, London, U.K., Jun. 1987, pp. 433–438.
- [10] W. Förstner and E. Gülch, "A fast operator for detection and precise location of distinct points, corners and centres of circular features," in *Proc. ISPRS Intercommission Workshop*, Interlaken, Switzerland, Jun. 1987, pp. 149–155.
- [11] J. Weickert, "A review of nonlinear diffusion filtering," in *Scale-Space Theory in Computer Vision*, ser. LNCS, B. ter Haar Romeny, L. Florack, J. Koenderink, and M. Viergever, Eds. Berlin, Germany: Springer, 1997, vol. 1252, pp. 260–271.
- [12] W. T. Freeman and E. H. Adelson, "The design and use of steerable filters," *IEEE Trans. Pattern Anal. Mach. Intell.*, vol. 13, no. 9, pp. 891–906, Sep. 1991.
- [13] H. Knutsson, R. Wilson, and G. H. Granlund, "Anisotropic nonstationary image estimation and its applications: Part I—Restoration of noisy images," *IEEE Trans. Commun.*, vol. COM-31, no. 3, pp. 388–397, Mar. 1983.
- [14] P. Perona and J. Malik, "Scale-space and edge detection using anisotropic diffusion," *IEEE Trans. Pattern Anal. Mach. Intell.*, vol. 12, no. 7, pp. 629–639, Jul. 1990.
- [15] J. Weickert, "Theoretical foundations of anisotropic diffusion in image processing," *Computing, Suppl.*, vol. 11, pp. 221–236, 1996.
- [16] R. van den Boomgaard, "Nonlinear diffusion in computer vision," Jan. 28, 2008 [Online]. Available: <http://staff.science.uva.nl/rein/nldiffusionweb/material.html>.
- [17] J. Weickert, K. Zuiderveld, B. ter Haar Romeny, and W. Niessen, "Parallel implementations of AOS schemes: A fast way of nonlinear diffusion filtering," in *Proc. IEEE Int. Conf. Image Process.*, 1997, pp. 396–399.
- [18] M. Welk, J. Weickert, and G. Steidl, "From tensor-driven diffusion to anisotropic wavelet shrinkage," in *Proc. Eur. Conf. Comput. Vis.*, 2006, vol. 3951, pp. 391–403.